

# Thermodynamic Interactions between Polystyrene and Long-Chain Poly(*n*-Alkyl Acrylates) Derived from Plant Oils

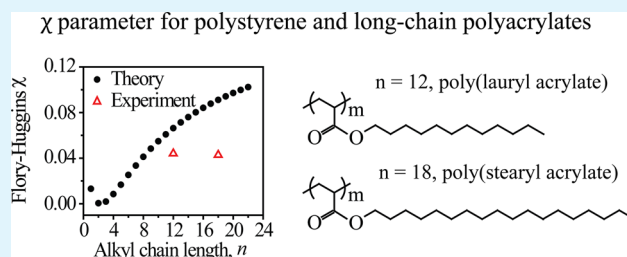
Shu Wang and Megan L. Robertson\*

Department of Chemical and Biomolecular Engineering, University of Houston, 4800 Calhoun Road, S222 Engineering Building 1, Houston, Texas 77204-4004, United States

## Supporting Information

**ABSTRACT:** Vegetable oils and their fatty acids are promising sources for the derivation of polymers. Long-chain poly(*n*-alkyl acrylates) and poly(*n*-alkyl methacrylates) are readily derived from fatty acids through conversion of the carboxylic acid end-group to an acrylate or methacrylate group. The resulting polymers contain long alkyl side-chains with around 10–22 carbon atoms. Regardless of the monomer source, the presence of alkyl side-chains in poly(*n*-alkyl acrylates) and poly(*n*-alkyl methacrylates) provides a convenient mechanism for tuning their physical properties. The development of structured multicomponent materials, including block copolymers and blends, containing poly(*n*-alkyl acrylates) and poly(*n*-alkyl methacrylates) requires knowledge of the thermodynamic interactions governing their self-assembly, typically described by the Flory–Huggins interaction parameter  $\chi$ . We have investigated the  $\chi$  parameter between polystyrene and long-chain poly(*n*-alkyl acrylate) homopolymers and copolymers: specifically we have included poly(stearyl acrylate), poly(lauryl acrylate), and their random copolymers. Lauryl and stearyl acrylate were chosen as model alkyl acrylates derived from vegetable oils and have alkyl side-chain lengths of 12 and 18 carbon atoms, respectively. Polystyrene is included in this study as a model petroleum-sourced polymer, which has wide applicability in commercially relevant multicomponent polymeric materials. Two independent methods were employed to measure the  $\chi$  parameter: cloud point measurements on binary blends and characterization of the order–disorder transition of triblock copolymers, which were in relatively good agreement with one another. The  $\chi$  parameter was found to be independent of the alkyl side-chain length (*n*) for large values of *n* (i.e., *n* > 10). This behavior is in stark contrast to the *n*-dependence of the  $\chi$  parameter predicted from solubility parameter theory. Our study complements prior work investigating the interactions between polystyrene and short-chain polyacrylates (*n* ≤ 10). To our knowledge, this is the first study to explore the thermodynamic interactions between polystyrene and long-chain poly(*n*-alkyl acrylates) with *n* > 10. This work lays the groundwork for the development of multicomponent structured systems (i.e., blends and copolymers) in this class of sustainable materials.

**KEYWORDS:** renewable resource polymers, poly(*n*-alkyl acrylates), poly(*n*-alkyl methacrylates), Flory–Huggins interaction parameter, alkyl chain length, side-chain, block copolymers, thermodynamic interactions



## INTRODUCTION

Vegetable oils and their fatty acids are promising replacements for petroleum sources for the derivation of polymers because of their abundance, low cost, lack of toxicity, biodegradability, and ease of functionalization that provides convenient routes to polymerization.<sup>1</sup> In one synthetic procedure, the carboxylic acid end-group of a fatty acid is converted to a hydroxyl group<sup>2</sup> and subsequently converted to an acrylate or methacrylate group, forming a long-chain *n*-alkyl acrylate or *n*-alkyl methacrylate.<sup>3</sup> Long-chain *n*-alkyl acrylates and *n*-alkyl methacrylates can be readily polymerized through free radical<sup>4–6</sup> or controlled radical<sup>7–10</sup> techniques to form poly(*n*-alkyl acrylates) and poly(*n*-alkyl methacrylates). When derived from fatty acids, the poly(*n*-alkyl acrylates) and poly(*n*-alkyl methacrylates) contain alkyl side-chains of length ranging between 10 and 22 carbon atoms, depending on the choice of fatty acid.<sup>1</sup>

Whether derived from plant or petroleum sources, the presence of side-chains in poly(*n*-alkyl acrylates) and poly(*n*-alkyl methacrylates) provides a convenient mechanism for tuning their physical properties. Previous studies by others have shown that the melting temperature, heat of fusion, crystallite size, gas permeability, and ultrasonic degradation rate of homopolymers and copolymers composed of poly(*n*-alkyl acrylates) and poly(*n*-alkyl methacrylates) are dependent on the alkyl side-chain length.<sup>4,11–17</sup> Our group has recently demonstrated that the melt viscosity of copolymers composed of long-chain poly(*n*-alkyl acrylates) is also dependent on the side-chain length.<sup>18</sup> Long-chain poly(*n*-alkyl acrylates) and poly(*n*-alkyl methacrylates) have been incorporated in a variety

Received: March 16, 2015

Accepted: April 29, 2015

Published: May 28, 2015

of classes of polymeric materials, including block copolymers,<sup>7,9,18–25</sup> thermoplastic elastomers,<sup>18,19</sup> pressure sensitive adhesives,<sup>26,27</sup> brushes,<sup>28</sup> and shape memory materials.<sup>29</sup>

The development of structured multicomponent materials, including block copolymers and blends, requires knowledge of the thermodynamic interactions governing their self-assembly. In this work, we focus on blends and block copolymers which contain long-chain poly(*n*-alkyl acrylates) and polystyrene. Polystyrene is chosen as a model component of these blends and copolymers to probe the impact of the length of the side-chain in the long-chain poly(*n*-alkyl acrylates) on the thermodynamic interactions between the material components. Polystyrene is a highly relevant petroleum-sourced polymer, employed in diverse multicomponent materials that contain polyolefins, polydienes, polyacrylates, and polymethacrylates, among others, making it an ideal candidate for fundamental studies on blend thermodynamics. The Flory–Huggins interaction parameter,  $\chi$ , (or the related binary interaction energy density) is traditionally employed to characterize the thermodynamic interactions between polymers.<sup>30,31</sup> The length of the side-chain of short-chain poly(*n*-alkyl acrylates) and poly(*n*-alkyl methacrylates) has been demonstrated to greatly influence their interactions with other polymers. Previous studies have characterized the  $\chi$  parameter between polystyrene and various short-chain poly(*n*-alkyl acrylates) using a variety of experimental techniques: cloud-point measurements or miscibility studies of blends,<sup>32,33</sup> the domain spacing of block copolymer melts,<sup>34</sup> melt titration,<sup>35</sup> and swelling experiments on interpenetrating networks.<sup>36,37</sup> A wider body of literature exists for the measurement of the  $\chi$  parameter between polystyrene and various short-chain poly(*n*-alkyl methacrylates), particularly for mixtures of polystyrene and poly(methyl methacrylate), employing cloud-point measurements or miscibility studies of blends,<sup>33,38–45</sup> small-angle neutron scattering,<sup>46–49</sup> neutron reflectivity,<sup>49,50</sup> solution behavior,<sup>51–53</sup> PVT experiments,<sup>40</sup> melt titration,<sup>35</sup> and swelling experiments on cross-linked polymers.<sup>54</sup> Furthermore, molecular dynamics simulations have been employed.<sup>55,56</sup>

Few studies have directly examined the influence of the side-chain length on the thermodynamic interactions between polystyrene and poly(*n*-alkyl acrylates) or poly(*n*-alkyl methacrylates), especially for large *n*. Two key studies have demonstrated that the solubility parameter of poly(*n*-alkyl acrylates) and poly(*n*-alkyl methacrylates) decreases with increasing alkyl chain length (*n*) for relatively short side-chain lengths (up to *n* = 10).<sup>32,57</sup> Systematic experimental measurements of the binary interaction energy density (which is directly related to the  $\chi$  parameter) with increasing *n* were not in agreement with that predicted from the solubility parameters.<sup>32</sup> Importantly, experimental measurements indicated that the binary interaction energy density increases only slightly when *n* increases from *n* = 4 to 10, in stark disagreement with the predictions from the solubility parameters.<sup>32</sup> To our knowledge, no previous studies have examined the thermodynamic interactions between polystyrene and long-chain poly(*n*-alkyl acrylates) or poly(*n*-alkyl methacrylates) (i.e., when *n* is greater than 10).

The objective of this work is to probe the influence of the alkyl side-chain length on the  $\chi$  parameter in the regime of long side-chain lengths (i.e., *n* > 10). Our model system contains polystyrene and long-chain poly(*n*-alkyl acrylate) homopolymers and copolymers: specifically, we have included poly(stearyl acrylate), poly(lauryl acrylate), and their random

copolymers. Lauryl and stearyl acrylate are derived from vegetable oils such as soybean, linseed, coconut, and palm kernel oils. For poly(lauryl acrylate) and poly(stearyl acrylate), the alkyl chain length, *n*, is 12 and 18, respectively. We have employed two experimental methods of characterizing the  $\chi$  parameter: cloud point measurements on binary blends and determination of the order–disorder transition temperature of triblock copolymers. The values of  $\chi(T)$  determined from both methods are compared, and the alkyl side-chain length-dependence of the  $\chi$  parameter is examined.

## ■ EXPERIMENTAL METHODS

**Materials.** All chemicals were purchased from Sigma-Aldrich unless otherwise noted below.

**Polymer Synthesis and Characterization.** Polystyrene (PS), poly(lauryl acrylate) [PLAc], poly(stearyl acrylate) [PSAc], poly(lauryl acrylate-*co*-stearyl acrylate) [poly(LAc-*co*-SAC)] random copolymers, and poly(styrene-*b*-(LAc-*co*-SAC)-*b*-styrene) (SAS) triblock copolymers were synthesized with reversible addition–fragmentation chain transfer polymerization, following procedures described in ref 18.

Molecular weight and molecular weight distribution (the dispersity, *D*) were characterized by a Viscotek gel permeation chromatography (GPC) instrument with Agilent ResiPore columns, using THF (OmniSolv, HPLC grade) as the mobile phase at 30 °C. The flow rate was 1 mL/min and the injection volume was 100  $\mu$ L. A triple detection system, including light scattering, a viscometer and refractometer, was employed to characterize the absolute molecular weight. Representative GPC chromatographs for the polymers used in this study are included in the Supporting Information (Figures S1–S4).

Proton nuclear magnetic resonance (<sup>1</sup>H NMR) experiments were performed on a JEOL ECA-500 instrument using deuterated chloroform (99.8 atom % D) as the solvent. <sup>1</sup>H NMR was utilized to determine the composition of the polyacrylate random copolymers and triblock copolymers (procedures are provided in ref 18). <sup>1</sup>H NMR was also used to characterize the relative proportions of meso and racemo dyads in the PLAc and PSAC homopolymers (evaluated following methods reported in refs,<sup>8,58</sup> and summarized in Figure S5 and Table S1 in the Supporting Information). PLAc and PSAC contained 39 and 36% meso dyads, respectively.

**Flory–Huggins Interaction Parameter.** Two methods were employed to characterize the Flory–Huggins interaction parameter ( $\chi$ ) between polystyrene and the polyacrylates: cloud point measurements and rheology.

**Cloud Point Measurements.** Films consisting of PS/PLAc (or PS/PSAc) blends were cast from dichloromethane solutions at room temperature on microscope slides. The films were allowed to air-dry and were subsequently dried in a vacuum oven at 150 °C for 4 h. The sample was covered by a second slide and sealed using 3M Scotch-Weld Epoxy Adhesive to avoid the thermal degradation of the polymers at elevated temperatures. The cloud point temperatures were determined through observing the optical character of the sample in a microscope (Olympus BXS1TRF) equipped with a heating cell (Instec HCS302-01). The sample temperature was first calibrated with a thermocouple and a calibration curve was constructed relating the sample temperature to the reported heating cell temperature. The sample was first heated to a temperature at which the blend was transparent, indicating the two polymers were miscible, and the sample was then cooled down slowly by 1 °C increment, and stabilized at each temperature for 2 min before observation of the sample with the microscope. The temperature at which the sample started to become opaque was identified as the cloud point temperature. The accuracy of the cloud point temperature is estimated to be within  $\pm 1$  °C for all experiments based on repeat measurements of the same sample. Experiments conducted upon heating to identify the location of the phase boundary were consistent with the results obtained upon cooling (observed difference was  $\leq 2$  °C).

**Rheology.** The order–disorder transition temperatures ( $T_{\text{ODT}}$ ) of SAS triblock copolymers were probed using a TA Instruments DHR-2 rheometer. A polymer disk with 25 mm diameter and 1 mm thickness was prepared by compression molding on a Carver Hotpress at an applied load of 4000 lbs at 210 °C. After cooling down to room temperature, the polymer disk was loaded between two 25 mm electrically heated parallel plates with a gap of around 1 mm. Nitrogen flowed continuously through the sample environment to avoid degradation of the polymer. The linear viscoelastic region was first determined using a strain sweep (1–50% strain) at a frequency of 10 rad/s. A frequency sweep was then completed (1–50 rad/s) using a strain in the linear region. This procedure was repeated upon cooling the sample from 300 to 30 °C (data were obtained at 10 °C intervals). The storage modulus at a frequency of 10 rad/s was plotted versus temperature, and the sharp decrease in storage modulus indicated the  $T_{\text{ODT}}$ , which is located as the intersection of two extrapolated lines. Multiple measurements were performed on the same sample to determine the error of the measurement, which was within  $\pm 1$  °C.

## DEFINITIONS

The thermodynamics of polymer blends and block copolymers are described by the following parameters: the composition of the block copolymer or blend, the Flory–Huggins interaction parameter ( $\chi$ ), and the number of repeat units of each component  $i$  in the blend or block copolymer ( $N_i$ ).<sup>59</sup> In this study,  $\chi$  and  $N_i$  are calculated based on a reference volume ( $v_{\text{ref}}$ ) of 100 Å<sup>3</sup>, following ref 60. The choice of a constant reference volume (and one that is independent of monomer type) allows for the most direct comparison of  $\chi$  parameters determined from blends containing polymers of varying molecular structure (and monomer volume). Furthermore,  $N_i$  is taken to be the weight-average degree of polymerization ( $N_{w,i}$ ) in the determination of  $\chi$  from cloud point measurements and number-average degree of polymerization ( $N_{n,i}$ ) in the determination of  $\chi$  from the order–disorder transition of triblock copolymers (refer to the Results for more details regarding the choice of molecular weight-average in these calculations). To define  $\chi$  and  $N_i$  based on  $v_{\text{ref}}$  we will use the following expressions:

$$N_{w,i} = \frac{v_{\text{mon},i} N_{\text{mon},i}}{v_{\text{ref}}} = \frac{M_{\text{mon},i}}{\rho_i N_A} \frac{M_{w,i}}{M_{\text{mon},i}} \frac{1}{v_{\text{ref}}} = \frac{M_{w,i}}{\rho_i N_A v_{\text{ref}}} \quad (1)$$

$$N_{n,i} = \frac{v_{\text{mon},i} N_{\text{mon},i}}{v_{\text{ref}}} = \frac{M_{\text{mon},i}}{\rho_i N_A} \frac{M_{n,i}}{M_{\text{mon},i}} \frac{1}{v_{\text{ref}}} = \frac{M_{n,i}}{\rho_i N_A v_{\text{ref}}} \quad (2)$$

In eqs 1 and 2,  $M_{\text{mon},i}$  is the molecular weight of a monomer repeat unit,  $v_{\text{mon},i}$  is the volume of a monomer repeat unit,  $N_{\text{mon},i}$  is the number of monomer repeat units on the polymer chain,  $M_{w,i}$  is the polymer weight-average molecular weight,  $M_{n,i}$  is the polymer number-average molecular weight,  $\rho_i$  is the polymer density, and  $N_A$  is Avogadro's number.

## RESULTS

**Temperature-Dependence of the Volume of a Monomer Repeat Unit ( $v_{\text{mon},i}$ ).** To employ eqs 1 and 2, the densities of the polyacrylates and PS are required. The PS density at room temperature was reported as 1.04 g/mL in ref 61. In a previous publication, we reported a procedure for measuring the densities of PLAc and poly(LAc-co-SAc) random copolymers, which were in the range of 0.92–0.94 g/mL at room temperature (around 21 °C).<sup>18</sup> Following the same procedure, the density of PSAc was measured to be 0.92 g/mL. With this information, the room temperature volume of a monomer repeat unit,  $v_{\text{mon},i}^{\circ}$  can be calculated as  $v_{\text{mon},i}^{\circ} =$

$(M_{\text{mon},i}/\rho_i N_A)$ . At elevated temperatures,  $v_{\text{mon},i}$  will be affected by the thermal expansion of the polymer, which can be calculated using the equation

$$v_{\text{mon},i}(T) = v_{\text{mon},i}^{\circ} [1 + \alpha_i (T - T^{\circ})] \quad (3)$$

where  $v_{\text{mon},i}^{\circ}$  is the monomer volume at room temperature,  $\alpha_i$  is the volumetric thermal expansion coefficient,  $T^{\circ}$  is room temperature, and  $T$  is the temperature of interest. The volumetric thermal expansion coefficient of PS has been reported to be  $2.16 \times 10^{-4}$  and  $5.13 \times 10^{-4} \text{ K}^{-1}$  for the glassy and rubbery states, respectively.<sup>62</sup> For PLAc, PSAc, and poly(LAc-co-SAc), there are no reported values to follow, however, Rogers et al. have studied the thermal expansion coefficients of a series of poly(*n*-alkyl methacrylates).<sup>63</sup> For PLAc and poly(LAc-co-SAc), the polymer is in a rubbery amorphous state at room temperature (the melting temperature,  $T_m$ , and the glass transition temperature,  $T_g$ , are below room temperature); the value of the thermal expansion coefficient is taken as that of poly(lauryl methacrylate) in the rubbery state ( $6.8 \times 10^{-4} \text{ K}^{-1}$ ).<sup>63</sup>

For the PSAc homopolymer, which has a  $T_m$  of around 50 °C,<sup>18</sup> the thermal expansion coefficients in the semicrystalline and amorphous states were taken to be those of poly(stearyl methacrylate) (PSMA) in the semicrystalline ( $4.0 \times 10^{-4} \text{ K}^{-1}$ ) and amorphous ( $6.2 \times 10^{-4} \text{ K}^{-1}$ ) states, respectively.<sup>63</sup> Additionally, there is a drastic increase in the specific volume during the melting transition. PSMA exhibited a 4.8% increase in specific volume upon melting;<sup>63</sup> this same increase in specific volume upon melting was applied to PSAc in our study.

For all polymers employed in this study, the temperature-dependent values of  $v_{\text{mon},i}$  were used to calculate the temperature-dependent volume fraction ( $\phi_i$ ) and  $N_i$  of each component in the blend or block copolymer. As the polymers utilized in this study have similar temperature-dependencies of  $v_{\text{mon},i}$ , the values of  $\phi_i$  did not vary significantly with temperature.

**Determination of the  $\chi$  Parameter from Cloud Point Measurements in Binary Blends.** Cloud point experiments were conducted on binary blends of PS and polyacrylate homopolymers. The homopolymer characteristics are summarized in Table 1. Blends were prepared as described in the

**Table 1. Characteristics of Homopolymers Used in Cloud Point Measurements<sup>a</sup>**

sample	$M_n$ (kg/mol)	$M_w$ (kg/mol)	$\bar{D}$	$N_w$ (at room temp.)
PS	3.1	3.4	1.11	55.7
PLAc	3.8	4.4	1.15	77.0
PSAc	2.5	2.6	1.05	46.6

<sup>a</sup> $M_n$ ,  $M_w$ , and  $\bar{D}$  were determined from GPC;  $N_w$  is the weight-average degree of polymerization (based on a reference volume of 100 Å<sup>3</sup> and using the room temperature densities of the polymers).

Experimental Methods with various compositions. The temperature at which the blend transitioned from transparent to opaque (i.e., the cloud point temperature,  $T_{\text{cp}}$ ) was determined using an optical microscope and the results are shown in Figure 1. The blend characteristics are summarized in Tables S2 and S3 of the Supporting Information.

The Flory–Huggins theory for the free energy of mixing of two homopolymers A and B is given by refs 30 and 31

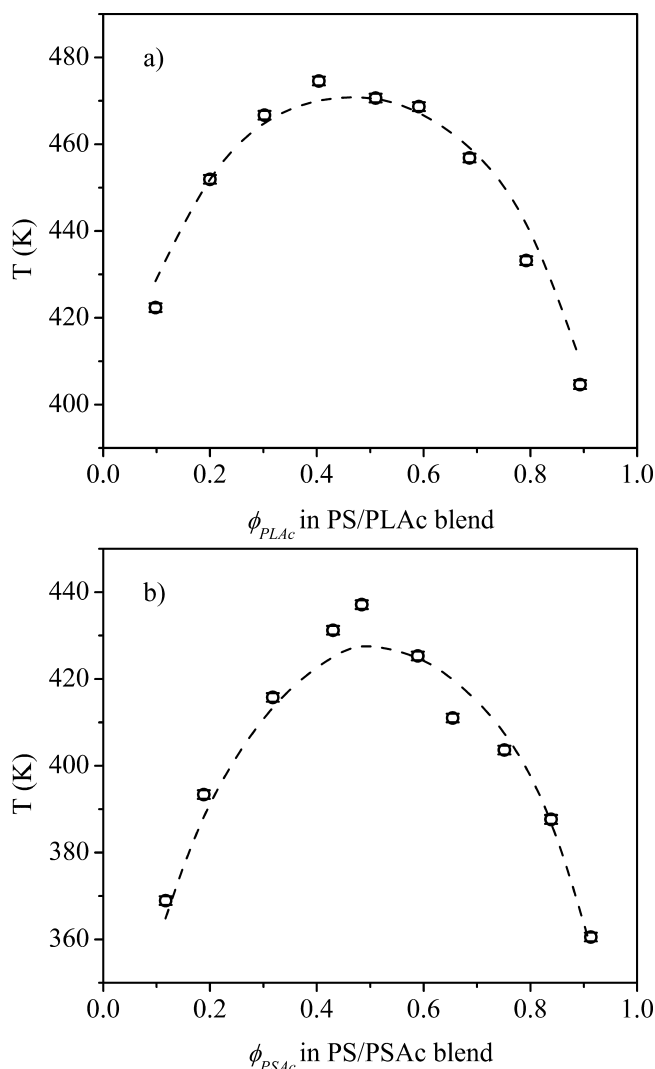


**Figure 1.** Cloud point temperatures (symbols) of (a) PS/PLAc blends and (b) PS/PSAc blends. The error bars for the cloud point temperature are included, and are approximately the size of the data points. The dashed curves represent the Flory–Huggins theory prediction of the location of the binodal curve, relying upon the results shown in Figure 2 and Figure S6 of the Supporting Information; procedures are described in the text.

$$\frac{\Delta G_m}{kT} = \frac{\phi_A \ln \phi_A}{v_{\text{mon},A} N_{\text{mon},A}} + \frac{\phi_B \ln \phi_B}{v_{\text{mon},B} N_{\text{mon},B}} + \chi \frac{\phi_A \phi_B}{v_{\text{ref}}} \quad (4)$$

where  $\Delta G_m$  is the free energy change on mixing per unit volume,  $k$  is the Boltzmann constant,  $T$  is the absolute temperature,  $\phi_i$  is the volume fraction of each blend component ( $i = A$  or  $B$ ),  $v_{\text{mon},i}$  is the volume of each monomer on chain  $i$ ,  $v_{\text{ref}}$  is the reference volume ( $100 \text{ \AA}^3$ ),  $N_{\text{mon},i}$  is the number of monomer repeat units in chain  $i$ , and  $\chi$  is the Flory–Huggins interaction parameter (based on the reference volume  $v_{\text{ref}}$ ).

Using eq 1, eq 4 can be rewritten as

$$\frac{\Delta G_m v_{\text{ref}}}{kT} = \frac{\phi_A \ln \phi_A}{N_{w,A}} + \frac{\phi_B \ln \phi_B}{N_{w,B}} + \chi \phi_A \phi_B \quad (5)$$

The binodal curve was constructed by deriving expressions for the chemical potentials of each component in the blend using eq 5 and equating the chemical potentials for each component in phases I and II:<sup>60</sup>

$$\ln \frac{\phi_A^I}{\phi_A^{II}} + (\phi_A^{II} - \phi_A^I) \left( 1 - \frac{N_{w,A}}{N_{w,B}} \right) + \chi N_{w,A} [(1 - \phi_A^I)^2 - (1 - \phi_A^{II})^2] = 0 \quad (6)$$

$$\ln \frac{1 - \phi_A^I}{1 - \phi_A^{II}} + (\phi_A^I - \phi_A^{II}) \left( 1 - \frac{N_{w,B}}{N_{w,A}} \right) + \chi N_{w,B} [(\phi_A^I)^2 - (\phi_A^{II})^2] = 0 \quad (7)$$

Simultaneously solving eqs 6 and 7 resulted in the determination of  $\phi_A^I$  and  $\phi_A^{II}$  as a function of  $\chi$ . The results of this calculation are shown in Figure S6 of the Supporting Information. We have chosen to use the weight-average degree of polymerization,  $N_w$ , in these calculations as larger sized molecules will drive the phase separation of polymer blends. A comparison of the cloud point data (Figure 1) and the theoretical binodal curve (Figure S6 of the Supporting Information) gives the relationship between  $\chi$  and  $T$ , reported in Figure 2.

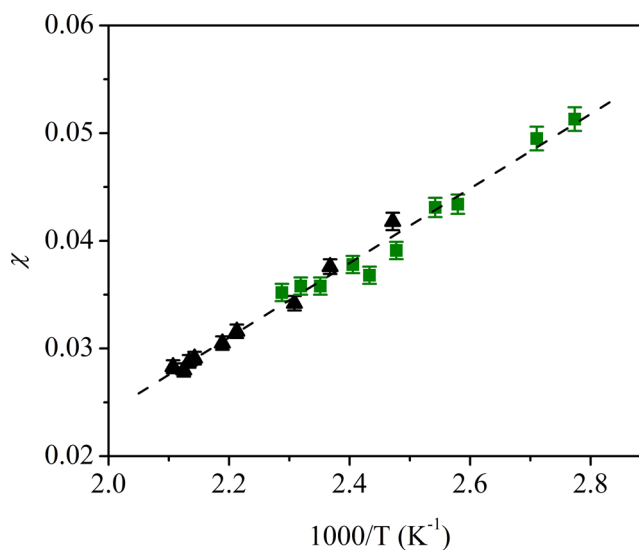


**Figure 2.**  $\chi$  as a function of inverse temperature for PS/polyacrylate blends from cloud point measurements: PS/PLAc binary blends (black  $\blacktriangle$ ); PS/PSAc binary blends (green  $\blacksquare$ ).  $\chi$  is based on a reference volume of  $100 \text{ \AA}^3$ . The error bars are included and in many cases are smaller than the data points. The data have been fit to a linear equation (dashed line):  $\chi = (34.6/T) - 0.0451$ .

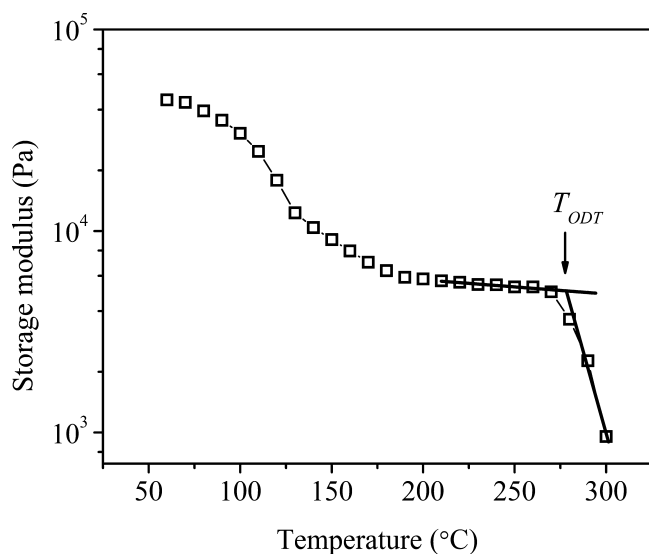
There are three categories of errors to consider in this measurement of  $\chi$ : (1) error in the molecular weight measurement from GPC, (2) error in the cloud point measurement, and (3) error in the thermal expansion coefficient. For the GPC measurement, the error has been found to be within  $\pm 2\%$  by multiple measurements. The error in cloud point measurement was within  $\pm 1 \text{ }^\circ\text{C}$  for all experiments. In this study, we do not quantify the error in the thermal expansion coefficient, which was taken from a literature source. The cumulative error is summarized in Tables S2 and S3 in the Supporting Information and shown as error bars in Figure 2. The  $\chi(T)$  curves for both polyacrylates are consistent with one another, indicating the behavior of  $\chi(T)$  is independent of the side chain length of polyacrylates.

Table 2. Characteristics of SAS Triblock Polymers Used in Rheology Measurements

polymer	$M_n$ (kg/mol) <sup>a</sup>	$\bar{D}$ <sup>a</sup>	$\phi_{PS}$ at room temp <sup>b</sup>	midblock $M_n$ (kg/mol) <sup>a</sup>	midblock $\bar{D}$ <sup>a</sup>	LAc wt % in midblock <sup>b</sup>
SAS(1-1)	76.2	1.67	0.230	57.3	1.26	100
SAS(1-2)	70.4	1.44	0.171	57.3	1.26	100
SAS(1-3)	48.7	1.38	0.180	39.2	NA <sup>c</sup>	100
SAS(2-1)	78.4	1.65	0.239	58.2	1.30	76
SAS(2-2)	72.3	1.43	0.180	58.2	1.30	76
SAS(2-3)	49.0	1.42	0.179	39.5	NA <sup>c</sup>	73
SAS(3-1)	75.7	1.61	0.231	56.8	1.28	61
SAS(3-2)	70.7	1.42	0.181	56.8	1.28	61
SAS(3-3)	48.3	1.44	0.181	38.8	NA <sup>c</sup>	62
SAS(4-1)	81.1	1.38	0.241	59.7	1.26	0
SAS(4-2)	73.2	1.44	0.167	59.7	1.26	0
SAS(4-3)	47.7	1.42	0.206	36.9	1.20	0
SAS(4-4)	70.7	1.38	0.141	59.7	1.26	0
SAS(4-5)	69.0	1.44	0.121	59.7	1.26	0

<sup>a</sup>Determined with GPC (light scattering). <sup>b</sup>Determined with <sup>1</sup>H NMR. <sup>c</sup>The triblock copolymer was synthesized through chain extension from PS (see ref 18) and the midblock  $\bar{D}$  cannot be measured.

**Determination of the  $\chi$  Parameter from the Order–Disorder Transition (ODT) of Triblock Copolymers.** Four series of triblock copolymers were investigated, with the polymer characteristics given in Table 2. The order–disorder transition temperatures ( $T_{ODT}$ ) of the polymers (determined through rheology as described in the Experimental Methods) are summarized in Table S4 of the Supporting Information. Figure 3 shows a representative data set, with the storage



**Figure 3.** Storage modulus as a function of temperature of triblock copolymer SAS(4-1). The  $T_{ODT}$  was determined as the intersection of the two extrapolated lines.<sup>64</sup>

modulus plotted as a function of temperature for SAS(4-1). The rheology data for the other samples are either provided in the Supporting Information (Figure S7) or, in some cases, were previously reported in ref 18.

The theoretical ODT of a triblock copolymer is defined by the composition (volume fraction of each block), and the thermodynamic parameter  $\chi N$ , where  $N$  is the number of total repeat units on the triblock copolymer (taken to be  $N_n$  in this study, following many prior studies on block copolymer thermodynamics).<sup>65</sup> With knowledge of the triblock copolymer  $N_n$  and composition, the predicted  $\chi$  value at the order–

disorder transition for each SAS triblock copolymer was calculated (Table S4 in the Supporting Information). Using the  $\chi$  value at the ODT and experimental  $T_{ODT}$  values, the relationship between  $T_{ODT}$  and  $\chi$  was constructed (additional information is provided in the Supporting Information).

There are still many open questions regarding the effects of dispersity on the block copolymer phase diagram.<sup>66</sup> We have chosen to compare  $\chi$  parameters calculated using two different theoretical triblock copolymer phase diagrams determined from self-consistent field theory: (1) the standard phase diagram of a monodisperse triblock copolymer, described in ref 65, and (2) the phase diagram for a triblock copolymer containing monodisperse end-blocks and a disperse midblock ( $\bar{D} = 1.5$ ), described in ref 67. Neither theoretical phase diagram is directly applicable to our SAS triblock copolymers, in which the polyacrylate midblock  $\bar{D} \approx 1.2-1.3$  (Table 2), the outerblock PS  $\bar{D} \approx 1.1$  (based upon characterization of PS homopolymers synthesized using the same methods), and the triblock copolymer molecular weight distribution is trimodal (described in more detail in ref 18).

Figure 4 and Table S4 in the Supporting Information show  $\chi$  versus  $1/T$  for SAS triblock copolymers of different midblock compositions (varying the wt % LAc in the midblock), using the theoretical phase diagram of a monodisperse triblock copolymer, taken from ref 65. The calculated  $\chi$  versus  $1/T$  using the phase diagram for a triblock copolymer containing a disperse midblock ( $\bar{D} = 1.5$ ), described in ref 67, is included in Figure S8 and Table S5 of the Supporting Information. Regardless of the theoretical phase diagram used in calculation of the  $\chi$  parameters, it is clear that the  $\chi(T)$  curves for all of the triblock copolymers are consistent with one another. The behavior of  $\chi(T)$  is thus independent of the midblock composition of the triblock copolymer.

The error in the  $\chi$  measurement was also evaluated and can be divided into four categories: (1) error in  $T_{ODT}$  from the rheology measurement, (2) error in molecular weight and volume fraction measurement from GPC and NMR, (3) error in the thermal expansion coefficient of each component, and (4) error in determining the theoretical  $\chi N$ . Multiple measurements of  $T_{ODT}$  have been taken on the same sample, and the error in  $T_{ODT}$  was within  $\pm 1$  °C. Multiple measurements of molecular weight and volume fraction were also performed and the errors for both were within  $\pm 2\%$ . We

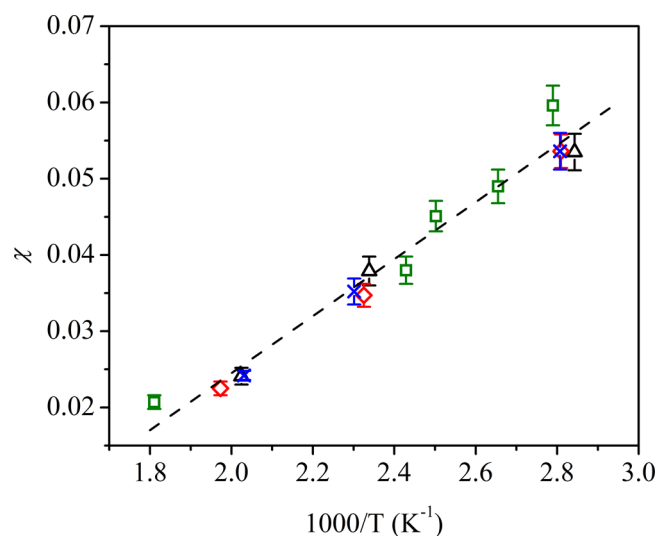


**Figure 4.**  $\chi$  as a function of inverse temperature determined from ODT measurements on SAS triblock copolymers (based on theoretical phase diagram in ref 65): 100% LAc in the midblock (black  $\Delta$ ); 76% LAc in the midblock (red  $\diamond$ ); 61% LAc in the midblock (blue  $\times$ ); 100% SAc in the midblock (green  $\square$ ).  $\chi$  is based on a reference volume of 100  $\text{\AA}^3$ . The error bars are included and in some cases are smaller than the data point. The data have been fit to a linear equation (dashed line):  $\chi = (37.4/T) - 0.0503$ .

are not able to evaluate the third category in this study, as we are drawing from the literature for the values of the thermal expansion coefficient. The uncertainty in determining  $\chi N$  from the theoretical phase diagram is potentially significant, and we have not attempted to quantify this error. Rather, in Figure S8 (Supporting Information), we have compared the results using two different theoretical phase diagrams of triblock copolymers with differing molecular weight distributions. The results from the first two categories of errors are summarized in Tables S4 and S5 of the Supporting Information and shown as error bars in Figure 4 and Figure S8 (Supporting Information).

## DISCUSSION

Figures 2 and 4 represent the temperature-dependent  $\chi$  parameters measured for PS and long-chain poly(*n*-alkyl acrylates). The poly(*n*-alkyl acrylates) included in this study are PLAc, PSAc, and poly(LAc-co-SAc) random copolymers. Importantly, the poly(*n*-alkyl acrylates) differ in the length of the side-chain on each repeat unit (12 and 18 carbon atoms for PLAc and PSAc, respectively).  $\chi$  parameters determined from cloud point measurements on binary blends and ODT measurements on triblock copolymers lie on one line in Figures 2 and 4 (within the error of the  $\chi$  measurement). This indicates that the length of the side-chain (*n*) of the polyacrylate has little effect on the thermodynamic interactions between PS and the poly(*n*-alkyl acrylates) at large values of *n*.

To explore the side-chain length-dependence of the  $\chi$  parameter, we have employed group contribution methods to calculate the solubility parameters ( $\delta$ ) of poly(*n*-alkyl acrylates) as a function of the side-chain length, *n*, shown in Figure 5. We have followed similar procedures to that described in ref 32 (using the van Krevelen parameters in ref 68). The results of our calculations are in good agreement with refs 57 and 32, which included side-chain lengths up to *n* = 10. Our calculations indicate that at higher values of *n* (>10), the solubility parameter continues to decrease slightly with

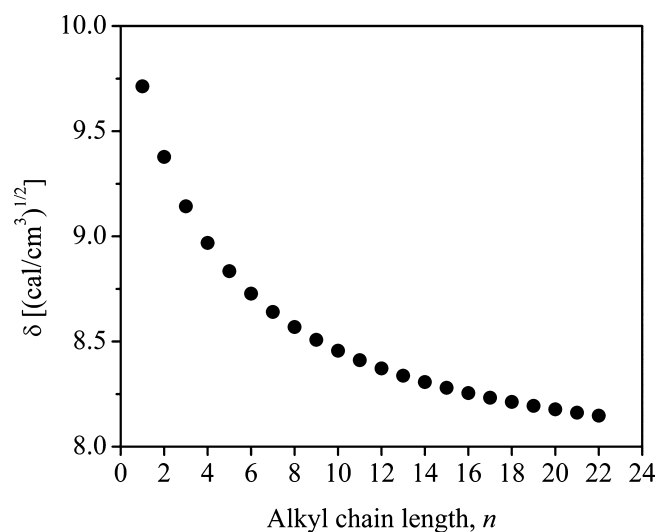


**Figure 5.** Solubility parameter ( $\delta$ ) of poly(*n*-alkyl acrylates) as a function of alkyl chain length (*n*).

increasing *n*. Additionally, we have calculated  $\delta$  of PS using the same methods ( $\delta = 9.3$ ).

The  $\chi$  parameter was calculated using eq 8

$$\chi = \frac{v_{\text{ref}}}{kT} (\delta_1 - \delta_2)^2 \quad (8)$$

where  $\delta_1$  and  $\delta_2$  are the solubility parameters of components 1 and 2, the reference volume was chosen to be 100  $\text{\AA}^3$ , and *k* is the Boltzmann constant.

Figure 6 compares the  $\chi$  parameter at 120 °C for PS and poly(*n*-alkyl acrylates) as a function of the alkyl side-chain

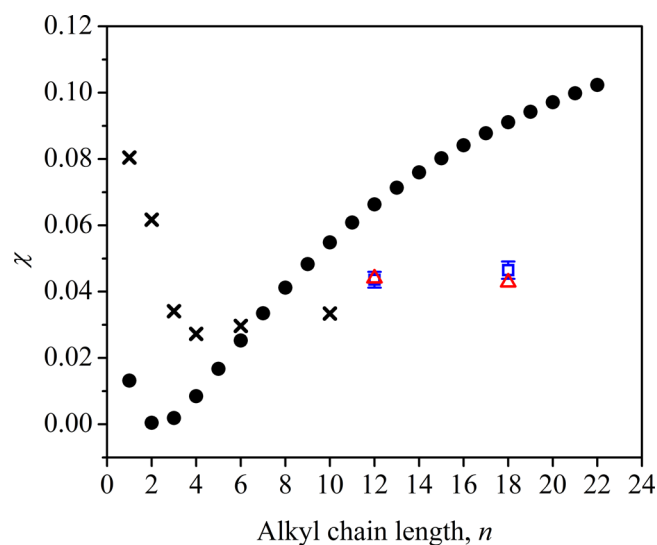


**Figure 6.** Effect of alkyl chain length on  $\chi$  of PS and poly(*n*-alkyl acrylates) ( $v_{\text{ref}} = 100 \text{\AA}^3$ ).  $\chi$  was calculated using solubility parameters (black  $\bullet$ ); calculated from binary interaction energy densities (determined by the copolymer/critical molecular weight method) reported in ref 32 (black  $\times$ ); and measured in this study through characterization of the ODT of triblock copolymers (blue  $\square$ ) and cloud point measurements on binary blends (red  $\Delta$ ). The error bars have been included for this study (*n* > 10): for the ODT measurements (blue  $\square$ ) the error bars are slightly larger than the data points and for the cloud point measurements (red  $\Delta$ ) they are smaller than the data points.

length,  $n$ . We have included  $\chi$  parameters in Figure 6 from three different sources: (1) calculated from the solubility parameters given in Figure 5 (using eq 8), (2) experimentally measured for short-chain poly( $n$ -alkyl acrylates), reported in ref 32 (we have calculated the  $\chi$  parameter using the binary interaction energy density reported in ref 32 and a reference volume of  $100 \text{ \AA}^3$ ), and (3) experimentally measured for long-chain poly( $n$ -alkyl acrylates) in our study (i.e., Figures 2 and 4). Additionally, in Figure S9 of the Supporting Information, the related binary interaction energy density is plotted as a function of  $n$  for the same polymer pairs.

It is clear that there are strong deviations between the  $\chi$  parameters calculated using solubility parameter theory and the experimentally measured values, consistent with the conclusions of ref 32 for poly( $n$ -alkyl acrylates) with  $n \leq 10$ . Other studies have compared the solubility parameters for a variety of polymers determined experimentally (i.e., through PVT measurements, scattering, cloud point experiments, inverse gas chromatography, among other methods) with those predicted from group contribution methods. In some cases there is good agreement,<sup>68–71</sup> and in other cases there are significant deviations between theory and experiment.<sup>68,72–74</sup> We also note that prediction of the  $\chi$  parameter from solubility parameter theory (regardless of the source of the solubility parameter) does not always agree with direct measurement of the  $\chi$  parameter, most notably in systems with a negative  $\chi$  parameter.<sup>75,76</sup> The results of our study indicate that group contribution methods, combined with solubility parameter theory, do not capture the thermodynamic behavior in blends of polystyrene and long-chain poly( $n$ -alkyl acrylates).

The experimentally measured  $\chi$  parameters reported in this manuscript are effective  $\chi$  parameters, which do not strictly follow the Flory–Huggins definition of  $\chi$ , but are fitting parameters that also account for additional contributions to the free energy of mixing not described by Flory–Huggins Theory. Oftentimes the empirical equation used in our study to describe the temperature-dependence of  $\chi$  ( $\chi = A/T + B$ ) is thought of in terms of an enthalpic contribution (i.e.,  $A/T$ ) and an entropic contribution (i.e.,  $B$ ). It may be more appropriate to directly compare the experimental enthalpic  $A/T$  term to the predictions from solubility parameter theory (i.e., eq 8). If we consider only the enthalpic  $A/T$  portion of our experimentally measured  $\chi(T)$  equations, we obtain similar values at  $120 \text{ }^\circ\text{C}$  for polyacrylates with  $n = 12$  and  $18$  ( $A/T = 0.095$  and  $0.090$  for PLAc and PSAc, respectively; refer to Figure S10 in the Supporting Information in which the data sets are analyzed separately). Though these values are closer in magnitude to the  $\chi$  parameters predicted by the group contribution methods for  $n = 12$  and  $18$  ( $0.066$  and  $0.091$  for PLAc and PSAc, respectively), there is still an important disconnect between the theory and experiment: the group contribution method predicts that  $\chi$  increases with increasing  $n$  (at high  $n$ ), whereas the experimental measurement (even when only considering the enthalpic  $A/T$  term) shows that  $\chi$  is independent of  $n$  (at high  $n$ ). Furthermore, the observation of a non-negligible  $B$  term is oftentimes associated with the presence of additional contributions to the entropy of mixing, such as differences in molecular packing of the pure component and mixed states. These effects may be important in these systems, but the magnitude of the  $B$  term in the  $\chi(T)$  equation is similar for polyacrylates with  $n = 12$  and  $18$  ( $B = -0.051$  and  $-0.047$  for PLAc and PSAc, respectively; refer to Figure S10 in the Supporting Information in which the data sets are analyzed

separately). Differences observed in the  $A$  and  $B$  parameters extracted for the fit of the  $\chi(T)$  equation to data obtained from each individual blend (or similarly, block copolymer), shown in Figure S10 of the Supporting Information, reflect the error of measuring  $\chi$  that has been quantified in this study.

The  $\chi$  parameter for PS and PLAc (or PSAc) was characterized using two independent methods: ODT measurements on triblock copolymers and cloud point measurements on binary blends. The  $\chi$  parameters determined from binary blends and block copolymers are quite similar to one another, though the level of quantitative agreement between them depends on the choice of theoretical phase diagram for the triblock copolymers (i.e., compare Figures S8a and S8b in the Supporting Information). The ability to generate a linear curve describing the temperature-dependence of  $\chi$  (i.e.,  $\chi = A/T + B$ ), as shown in Figures 2 and 4, through measurements on blends and block copolymers of varying composition, which contain polymers of varying molecular weight, indicates that these  $\chi$  parameters are relatively insensitive to molecular weight and composition effects.

Importantly, we can conclude that at longer side-chain lengths ( $n > 10$ ), the  $\chi$  parameter is independent of the alkyl side-chain length,  $n$ . To our knowledge, this is the first study to explore the thermodynamic interactions between PS and long-chain poly( $n$ -alkyl acrylates) with  $n > 10$ . The characterization of the Flory–Huggins interaction parameter is an essential first step to the design of microstructured or nanostructured materials in multicomponent systems, guided by predictions of theories, such as self-consistent field theory.<sup>77–79</sup> Importantly, our work highlights the necessity for alternative theories to understand the origins of the behavior in this class of materials.

## CONCLUSIONS

Two independent methods were employed to calculate the Flory–Huggins interaction parameter ( $\chi$ ) between polystyrene (PS) and long-chain poly( $n$ -alkyl acrylates): cloud point measurements on binary blends and characterization of the order–disorder transition of triblock copolymers. The poly( $n$ -alkyl acrylates) included in this study were poly(lauryl acrylate) (PLAc), poly(stearyl acrylate) (PSAc), and poly(LAc-co-SAc) random copolymers. Importantly, the poly( $n$ -alkyl acrylates) differ in the length of the alkyl side-chain on each repeat unit ( $12$  and  $18$  carbon atoms for PLAc and PSAc, respectively). The  $\chi$  parameter was found to be independent of the alkyl side-chain length ( $n$ ) for large values of  $n$ . This behavior is in stark contrast to the  $n$ -dependence of the  $\chi$  parameter predicted from solubility parameter theory. To our knowledge, this is the first study to explore the thermodynamic interactions between PS and long-chain poly( $n$ -alkyl acrylates) with  $n > 10$ . In addition, the  $\chi$  parameter appears to be relatively insensitive to polymer chain architecture, molecular weight, and composition in this system, as the temperature-dependence of the  $\chi$  parameter was extracted from blends and block copolymers in which all of these parameters were varying. This work lays the foundation for future studies to examine blends or block copolymers consisting of long-chain poly( $n$ -alkyl acrylates) and various other constituents, including the examination of systems containing multiple components with long side-chains. The implementation of polymers derived from fatty acids and vegetable oils in multicomponent materials, such as blends and copolymers, will rely upon a detailed understanding of the thermodynamic interactions in such systems.

## ■ ASSOCIATED CONTENT

## ■ Supporting Information

Representative GPC traces for a SAS triblock copolymer (Figure S1), PLAc used in cloud point measurements (Figure S2), PSAc used in cloud point measurements (Figure S3), and PS used in cloud point measurements (Figure S4); NMR data and characterization of meso and racemo dyads in PLAc and PSAc (Figure S5 and Table S1); cloud point blend characteristics and results (Tables S2 and S3); Flory–Huggins theory prediction of the binodal curve  $\chi$  vs composition in binary blends (Figure S6); storage modulus as a function of temperature used in the ODT determination of SAS triblock copolymers (Figure S7); summary of  $\chi$  parameters determined from rheology measurements (Tables S4 and S5); comparison of  $\chi(T)$  from different methods (Figure S8); binary interaction energy density as a function of alkyl side-chain length (Figure S9); and linear fit of  $\chi(T)$  using data sets for each individual sample and characterization method (Figure S10). The Supporting Information is available free of charge on the ACS Publications website at DOI: 10.1021/acsami.5b02326.

## ■ AUTHOR INFORMATION

## Corresponding Author

\*E-mail: mlrobertson@uh.edu. Phone: 713-743-2748.

## Notes

The authors declare no competing financial interest.

## ■ ACKNOWLEDGMENTS

The authors appreciate the assistance of Dr. Charles Anderson for access and training in the University of Houston Department of Chemistry Nuclear Magnetic Resonance Facility. We are grateful to Dr. Ramanan Krishnamoorti and Dr. Nathaniel A. Lynd for helpful discussions. This material is based upon work supported by the National Science Foundation under Grant No. DMR-1351788. The authors also thank the University of Houston for start-up funds.

## ■ REFERENCES

- (1) Meier, M. A. R.; Metzger, J. O.; Schubert, U. S. Plant Oil Renewable Resources as Green Alternatives in Polymer Science. *Chem. Soc. Rev.* **2007**, *36*, 1788–1802.
- (2) Voeste, T.; Buchold, H. Production of Fatty Alcohols from Fatty Acids. *J. Am. Oil Chem. Soc.* **1984**, *61* (2), 350–352.
- (3) Dutta, P.; Gogoi, B.; Dass, N. N.; Sen Sarma, N. Efficient Organic Solvent and Oil Sorbent Co-Polyesters: Poly-9-octadecenylacrylate/Methacrylate with 1-Hexene. *React. Funct. Polym.* **2013**, *73* (3), 457–464.
- (4) O'Leary, K.; Paul, D. R. Copolymers of Poly(N-Alkyl Acrylates): Synthesis, Characterization, and Monomer Reactivity Ratios. *Polymer* **2004**, *45* (19), 6575–6585.
- (5) Charton, N.; Feldermann, A.; Theis, A.; Stenzel, M. H.; Davis, T. P.; Barner-Kowollik, C. Initiator Efficiency of 2,2'-Azobis-(Isobutyronitrile) in Bulk Dodecyl Acrylate Free-Radical Polymerizations over a Wide Conversion and Molecular Weight Range. *J. Polym. Sci., Polym. Chem.* **2004**, *42* (20), S170–S179.
- (6) Lovestead, T. M.; Davis, T. P.; Stenzel, M. H.; Barner-Kowollik, C. Scope for Accessing the Chain Length Dependence of the Termination Rate Coefficient for Disparate Length Radicals in Acrylate Free Radical Polymerization. *Macromol. Symp.* **2007**, *248*, 82–93.
- (7) Chatterjee, D. P.; Mandal, B. M. Facile Atom Transfer Radical Homo and Block Copolymerization of Higher Alkyl Methacrylates at Ambient Temperature Using CuCl/PMDETA/Quaternary Ammonium Halide Catalyst System. *Polymer* **2006**, *47* (6), 1812–1819.

- (8) Coelho, J. F. J.; Carvalho, E. Y.; Marques, D. S.; Popov, A. V.; Goncalves, P. M.; Gil, M. H. Synthesis of Poly(Lauryl Acrylate) by Single-Electron Transfer/Degenerative Chain Transfer Living Radical Polymerization Catalyzed by Na<sub>2</sub>S<sub>2</sub>O<sub>4</sub> in Water. *Macromol. Chem. Phys.* **2007**, *208* (11), 1218–1227.

- (9) Dutertre, F.; Pennarun, P.-Y.; Colombani, O.; Nicol, E. Straightforward Synthesis of Poly(Lauryl Acrylate)-*b*-Poly(Stearyl Acrylate) Diblock Copolymers by ATRP. *Eur. Polym. J.* **2011**, *47* (3), 343–351.

- (10) Theis, A.; Feldermann, A.; Charton, N.; Davis, T. P.; Stenzel, M. H.; Barner-Kowollik, C. Living Free Radical Polymerization (RAFT) of Dodecyl Acrylate: Chain Length Dependent Termination, Mid-Chain Radicals and Monomer Reaction Order. *Polymer* **2005**, *46* (18), 6797–6809.

- (11) O'Leary, K. A.; Paul, D. R. Physical Properties of Poly(*n*-Alkyl Acrylate) Copolymers. Part 2. Crystalline/Non-Crystalline Combinations. *Polymer* **2006**, *47* (4), 1245–1258.

- (12) O'Leary, K. A.; Paul, D. R. Physical Properties of Poly(*n*-Alkyl Acrylate) Copolymers. Part 1. Crystalline/Crystalline Combinations. *Polymer* **2006**, *47* (4), 1226–1244.

- (13) Jordan, E. F. Side-Chain Crystallinity. III. Influence of Side-Chain Crystallinity on the Glass Transition Temperatures of Selected Copolymers Incorporating *n*-Octadecyl Acrylate or Vinyl Stearate. *J. Polym. Sci., Part A: Polym. Chem.* **1971**, *9* (11), 3367–3378.

- (14) Jordan, E. F.; Artymyshyn, B.; Specca, A.; Wrigley, A. N. Side-Chain Crystallinity. II. Heats of Fusion and Melting Transitions on Selected Copolymers Incorporating *n*-Octadecyl Acrylate or Vinyl Stearate. *J. Polym. Sci., Part A: Polym. Chem.* **1971**, *9* (11), 3349–3365.

- (15) Jordan, E. F.; Feldeise, D. W.; Wrigley, A. N. Side-Chain Crystallinity. I. Heats of Fusion and Melting Transitions on Selected Homopolymers Having Long Side Chains. *J. Polym. Sci., Part A: Polym. Chem.* **1971**, *9* (7), 1835–1851.

- (16) Mahalik, J. P.; Madras, G. Effect of Alkyl Group Substituents, Temperature, and Solvents on the Ultrasonic Degradation of Poly(*n*-Alkyl Acrylates). *Ind. Eng. Chem. Res.* **2005**, *44* (17), 6572–6577.

- (17) Prasad, S.; Jiang, Z.; Sinha, S. K.; Dhinojwala, A. Partial Crystallinity in Alkyl Side Chain Polymers Dictates Surface Freezing. *Phys. Rev. Lett.* **2008**, *101* (6), No. 065505.

- (18) Wang, S.; Vajjala Kesava, S.; Gomez, E. D.; Robertson, M. L. Sustainable Thermoplastic Elastomers Derived from Fatty Acids. *Macromolecules* **2013**, *46* (18), 7202–7212.

- (19) Chatterjee, D. P.; Mandal, B. M. Triblock Thermoplastic Elastomers with Poly(Lauryl Methacrylate) as the Center Block and Poly(Methyl Methacrylate) or Poly(Tert-Butyl Methacrylate) as End Blocks. Morphology and Thermomechanical Properties. *Macromolecules* **2006**, *39* (26), 9192–9200.

- (20) Karky, K.; Clisson, G.; Reiter, G.; Billon, L. Semicrystalline Macromolecular Design by Nitroxide-Mediated Polymerization. *Macromol. Chem. Phys.* **2008**, *209* (7), 715–722.

- (21) Penfold, H. V.; Holder, S. J.; McKenzie, B. E. Octadecyl Acrylate–Methyl Methacrylate Block and Gradient Copolymers from ATRP: Comb-Like Stabilizers for the Preparation of Micro- and Nanoparticles of Poly(Methyl Methacrylate) and Poly(Acrylonitrile) by Non-Aqueous Dispersion Polymerization. *Polymer* **2010**, *51* (9), 1904–1913.

- (22) Qin, S. H.; Saget, J.; Pyun, J. R.; Jia, S. J.; Kowalewski, T.; Matyjaszewski, K. Synthesis of Block, Statistical, and Gradient Copolymers from Octadecyl (Meth)Acrylates Using Atom Transfer Radical Polymerization. *Macromolecules* **2003**, *36* (24), 8969–8977.

- (23) Richard, R. E.; Schwarz, M.; Ranade, S.; Chan, A. K.; Matyjaszewski, K.; Sumerlin, B. Evaluation of Acrylate-Based Block Copolymers Prepared by Atom Transfer Radical Polymerization as Matrices for Paclitaxel Delivery from Coronary Stents. *Biomacromolecules* **2005**, *6* (6), 3410–3418.

- (24) Wu, W.; Huang, J. Y.; Jia, S. J.; Kowalewski, T.; Matyjaszewski, K.; Pakula, T.; Gitsas, A.; Floudas, G. Self-Assembly of PODMA-*b*-PtBA-*b*-PODMA Triblock Copolymers in Bulk and on Surfaces. A Quantitative SAXS/AFM Comparison. *Langmuir* **2005**, *21* (21), 9721–9727.



- (25) Zhu, X. L.; Gu, Y. R.; Chen, G. J.; Cheng, Z. P.; Lu, J. M. Synthesis of Poly(Octadecyl Acrylate-*b*-Styrene-*b*-Octadecyl Acrylate) Triblock Copolymer by Atom Transfer Radical Polymerization. *J. Appl. Polym. Sci.* **2004**, *93* (4), 1539–1545.
- (26) Agirre, A.; de las Heras-Alarcon, C.; Wang, T.; Keddie, J. L.; Asua, J. M. Waterborne, Semicrystalline, Pressure-Sensitive Adhesives with Temperature-Responsiveness and Optimum Properties. *ACS Appl. Mater. Interfaces* **2010**, *2* (2), 443–451.
- (27) Agirre, A.; Nase, J.; Degrandi, E.; Creton, C.; Asua, J. M. Improving Adhesion of Acrylic Waterborne PSAs to Low Surface Energy Materials: Introduction of Stearyl Acrylate. *J. Polym. Sci., Part A: Polym. Chem.* **2010**, *48* (22), 5030–5039.
- (28) Öztürk, E.; Turan, E.; Caykara, T. Fabrication of Ultrahydrophobic Poly(Lauryl Acrylate) Brushes on Silicon Wafer Via Surface-Initiated Atom Transfer Radical Polymerization. *Appl. Surf. Sci.* **2010**, *257* (3), 1015–1020.
- (29) Fei, P.; Cavicchi, K. A. Synthesis and Characterization of a Poly(Styrene-Block-Methylacrylate-Random-Octadecylacrylate-Block-Styrene) Shape Memory ABA Triblock Copolymer. *ACS Appl. Mater. Interfaces* **2010**, *2* (10), 2797–2803.
- (30) Flory, P. J. Thermodynamics of High Polymer Solutions. *J. Chem. Phys.* **1942**, *10* (1), 51–61.
- (31) Huggins, M. L. Some Properties of Solutions of Long-Chain Compounds. *J. Phys. Chem.* **1942**, *46* (1), 151–158.
- (32) Zhu, S.; Paul, D. R. Binary Interaction Energy Densities for Blends of Styrene/Acrylonitrile Copolymers with Methyl Methacrylate/*n*-Alkyl Acrylate Copolymers. *Macromolecules* **2002**, *35* (21), 8227–8238.
- (33) Chu, J. H.; Paul, D. R. Interaction Energies for Blends of SAN with Methyl Methacrylate Copolymers with Ethyl Acrylate and *n*-Butyl Acrylate. *Polymer* **1999**, *40* (10), 2687–2698.
- (34) Men'shikov, E. A.; Bol'shakova, A. V.; Yaminskii, I. V. Determination of the Flory–Huggins Parameter for a Pair of Polymer Units from AFM Data for Thin Films of Block Copolymers. *Prot. Met. Phys. Chem. Surf.* **2009**, *45* (3), 295–299.
- (35) Somani, R. H.; Shaw, M. T. Miscibility of Acrylic Polymers in Polystyrene by Melt Titration. *Macromolecules* **1981**, *14* (5), 1549–1554.
- (36) Sperling, L. H.; Widmaier, J. M. A Survey of Dual Phase Continuity and Miscibility in Interpenetrating Polymer Networks, Making Use of Selective Decrosslinking and Dissolution of One Component: Poly(*n*-Butyl Acrylate)/Polystyrene. *Polym. Eng. Sci.* **1983**, *23* (12), 693–696.
- (37) Widmaier, J. M.; Sperling, L. H. A Comparative Study of Semi-2 and Full Interpenetrating Polymer Networks Based on Poly(*n*-Butyl Acrylate)/Polystyrene. *J. Appl. Polym. Sci.* **1982**, *27* (9), 3513–3525.
- (38) Callaghan, T. A.; Paul, D. R. Interaction Energies for Blends of Poly(Methyl Methacrylate), Polystyrene, and Poly(Alpha-Methylstyrene) by the Critical Molecular Weight Method. *Macromolecules* **1993**, *26* (10), 2439–2450.
- (39) Chu, J. H.; Tilakaratne, H. K.; Paul, D. R. Blends of Tribromostyrene Copolymers. *Polymer* **2000**, *41* (14), 5393–5403.
- (40) Kressler, J.; Higashida, N.; Shimomai, K.; Inoue, T.; Ougizawa, T. Temperature Dependence of the Interaction Parameter between Polystyrene and Poly(Methyl Methacrylate). *Macromolecules* **1994**, *27* (9), 2448–2453.
- (41) Zhu, S.; Paul, D. R. Evaluation of the Styrene/*n*-Butyl Methacrylate Binary Interaction Energy Density. *Polymer* **2003**, *44* (14), 3963–3968.
- (42) Zhu, S.; Paul, D. R. Re-Examination of the Miscibility Behavior of Smma Copolymers Using Various Techniques. *Polymer* **2003**, *44* (10), 3009–3019.
- (43) Browarzik, D. Calculation of the Phase Behavior of Polystyrene/Poly(*n*-Pentyl Methacrylate) Blends. *J. Macromol. Sci., Part A* **2005**, *42* (10), 1339–1353.
- (44) Ryu, D. Y.; Lee, D. H.; Jeong, U.; Yun, S. H.; Park, S.; Kwon, K.; Sohn, B. H.; Chang, T.; Kim, J. K.; Russell, T. P. Closed-Loop Phase Behavior of Polystyrene-Block-Poly(*n*-Pentyl Methacrylate) Copolymers with Various Block Length Ratios. *Macromolecules* **2004**, *37* (10), 3717–3724.
- (45) Sato, T.; Ikeda, M.; Sugawara, A. Effect of Monomer Sequence on Miscibility in Statistical Copolymer Blends and Estimation of Segmental X Parameters from Their Miscibility. *Polym. Int.* **2004**, *53* (7), 951–958.
- (46) Cho, J. Hartree Analysis of Chi for a Pressure-Responsive Diblock Copolymer: Temperature-Pressure Superposition. *Macromol. Res.* **2012**, *20* (5), 534–539.
- (47) Russell, T. P.; Hjelm, R. P.; Seeger, P. A. Temperature Dependence of the Interaction Parameter of Polystyrene and Poly(Methyl Methacrylate). *Macromolecules* **1990**, *23* (3), 890–893.
- (48) Hammouda, B.; Bauer, B. J.; Russell, T. P. Small-Angle Neutron Scattering from Deuterated Polystyrene/Poly(Butyl Methacrylate) Homopolymer Blend Mixtures. *Macromolecules* **1994**, *27* (8), 2357–2359.
- (49) Schubert, D. W.; Abetz, V.; Stamm, M.; Hack, T.; Siol, W. Composition and Temperature Dependence of the Segmental Interaction Parameter in Statistical Copolymer/Homopolymer Blends. *Macromolecules* **1995**, *28* (7), 2519–2525.
- (50) Siqueira, D. F.; Schubert, D. W.; Erb, V.; Stamm, M.; Amato, J. P. Interface Thickness of the Incompatible Polymer System Ps/PNBMA as Measured by Neutron Reflectometry and Ellipsometry. *Colloid Polym. Sci.* **1995**, *273* (11), 1041–1048.
- (51) Fukuda, T.; Inagaki, H. Interactions between Unlike Polymers Versus Dilute Solution Properties of Copolymers. *Pure Appl. Chem.* **1983**, *55* (10), 1541–1551.
- (52) Geveke, D. J.; Danner, R. P. Ternary Phase Equilibria of Polystyrene with a Second Polymer and a Solvent. *J. Appl. Polym. Sci.* **1993**, *47* (4), 565–575.
- (53) Sun, Z.; Wang, C. H. Quasielastic Light Scattering from Semidilute Ternary Polymer Solutions of Polystyrene and Poly-(Methyl Methacrylate) in Benzene. *Macromolecules* **1996**, *29* (6), 2011–2018.
- (54) Durant, Y. G.; Sundberg, D. C.; Guillot, J. A Comparison of Methods for the Estimation of Polymer Monomer Interaction Parameters—The Polystyrene *n*-Butyl Methacrylate System. *J. Appl. Polym. Sci.* **1994**, *52* (12), 1823–1832.
- (55) Ahmadi, A.; Freire, J. J. Molecular Dynamics Simulation of Miscibility in Several Polymer Blends. *Polymer* **2009**, *50* (20), 4973–4978.
- (56) Mu, D.; Li, J. Q.; Zhou, Y. H. Modeling and Analysis of the Compatibility of Polystyrene/Poly(Methyl Methacrylate) Blends with Four Inducing Effects. *J. Mol. Model* **2011**, *17* (3), 607–619.
- (57) Lewin, J. L.; Maerzke, K. A.; Schultz, N. E.; Ross, R. B.; Siepmann, J. I. Prediction of Hildebrand Solubility Parameters of Acrylate and Methacrylate Monomers and their Mixtures by Molecular Simulation. *J. Appl. Polym. Sci.* **2010**, *116* (1), 1–9.
- (58) Tabuchi, M.; Kawachi, T.; Kitayama, T.; Hatada, K. Living Polymerization of Primary Alkyl Acrylates with *t*-Butyllithium/Bulky Aluminum Lewis Acids. *Polymer* **2002**, *43* (25), 7185–7190.
- (59) Matsen, M. W.; Bates, F. S. Block Copolymer Microstructures in the Intermediate-Segregation Regime. *J. Chem. Phys.* **1997**, *106* (6), 2436–2448.
- (60) Eitouni, H. B.; Balsara, N. P. Thermodynamics of Polymer Blends. In *Physical Properties of Polymers Handbook*, 2nd ed.; Mark, J. E., Ed. Springer: New York, 2007.
- (61) Choy, C. L.; Hunt, R. G.; Salinger, G. L. Specific Heat of Amorphous Polymethyl Methacrylate and Polystyrene Below 4 K. *J. Chem. Phys.* **1970**, *52* (7), 3629–3633.
- (62) Quach, A.; Simha, R. Pressure–Volume–Temperature Properties and Transitions of Amorphous Polymers: Polystyrene and Poly(Orthomethylstyrene). *J. Appl. Phys.* **1971**, *42* (12), 4592–4606.
- (63) Rogers, S.; Mandelkern, L. Glass Transitions of the Poly(*n*-Alkyl Methacrylates). *J. Phys. Chem.* **1957**, *61* (7), 985–991.
- (64) Lynd, N. A.; Hillmyer, M. A. Effects of Polydispersity on the Order–Disorder Transition in Block Copolymer Melts. *Macromolecules* **2007**, *40* (22), 8050–8055.

(65) Matsen, M. W. Effect of Architecture on the Phase Behavior of AB-Type Block Copolymer Melts. *Macromolecules* **2012**, *45* (4), 2161–2165.

(66) Lynd, N. A.; Meuler, A. J.; Hillmyer, M. A. Polydispersity and Block Copolymer Self-Assembly. *Prog. Polym. Sci.* **2008**, *33* (9), 875–893.

(67) Matsen, M. W. Comparison of A-Block Polydispersity Effects on BAB Triblock and AB Diblock Copolymer Melts. *Eur. Phys. J. E: Soft Matter Biol. Phys.* **2013**, *36* (4), 1–7.

(68) Van Krevelen, D. W.; Te Nijenhuis, K. Chapter 7: Cohesive Properties and Solubility. In *Properties of Polymers*, 4th ed.; Van Krevelen, D. W., Te Nijenhuis, K., Eds.; Elsevier: Amsterdam, 2009; pp 189–227.

(69) D'Amelia, R. P.; Tomic, J. C.; Nirode, W. F. The Determination of the Solubility Parameter ( $\Delta$ ) and the Mark-Houwink Constants ( $K$  &  $\alpha$ ) of Food Grade Polyvinyl Acetate (PVAC). *J. Polym. Biopolym. Phys. Chem.* **2014**, *2* (4), 67–72.

(70) Liu, Y.; Shi, B. L. Determination of Flory Interaction Parameters between Polyimide and Organic Solvents by HSP Theory and IGC. *Polym. Bull.* **2008**, *61* (4), 501–509.

(71) Bordes, C.; Freville, V.; Ruffin, E.; Marote, P.; Gauvrit, J. Y.; Briancon, S.; Lanteri, P. Determination of Poly(Epsilon-Caprolactone) Solubility Parameters: Application to Solvent Substitution in a Microencapsulation Process. *Int. J. Pharm.* **2010**, *383* (1–2), 236–243.

(72) Graessley, W. W.; Krishnamoorti, R.; Balsara, N. P.; Fetters, L. J.; Lohse, D. J.; Schulz, D. N.; Sissano, J. A. Deuteration Effects and Solubility Parameter Ordering in Blends of Saturated Hydrocarbon Polymers. *Macromolecules* **1994**, *27* (9), 2574–2579.

(73) Kim, S. D.; Chakravarti, S.; Tian, J.; Bell, P. The Phase Behavior and the Flory–Huggins Interaction Parameter of Blends Containing Amorphous Poly(Resorcinol Phthalate-Block-Carbonate), Poly(Bisphenol-A Carbonate) and Poly(Ethylene Terephthalate). *Polymer* **2010**, *51* (10), 2199–2206.

(74) Cochran, E. W.; Bates, F. S. Thermodynamic Behavior of Poly(Cyclohexylethylene) in Polyolefin Diblock Copolymers. *Macromolecules* **2002**, *35* (19), 7368–7374.

(75) Graessley, W. W.; Krishnamoorti, R.; Reichart, G. C.; Balsara, N. P.; Fetters, L. J.; Lohse, D. J. Regular and Irregular Mixing in Blends of Saturated Hydrocarbon Polymers. *Macromolecules* **1995**, *28* (4), 1260–1270.

(76) Krishnamoorti, R.; Graessley, W. W.; Fetters, L. J.; Garner, R. T.; Lohse, D. J. Anomalous Mixing Behavior of Polyisobutylene with Other Polyolefins. *Macromolecules* **1995**, *28* (4), 1252–1259.

(77) Helfand, E. Theory of Inhomogeneous Polymers: Fundamentals of the Gaussian Random-Walk Model. *J. Chem. Phys.* **1975**, *62* (3), 999–1005.

(78) Evers, O. A.; Scheutjens, J. M. H. M.; Fleer, G. J. Statistical Thermodynamics of Block Copolymer Adsorption. 1. Formulation of the Model and Results for the Adsorbed Layer Structure. *Macromolecules* **1990**, *23* (25), 5221–5233.

(79) Matsen, M. W. The Standard Gaussian Model for Block Copolymer Melts. *J. Phys.: Cond. Matt.* **2002**, *14* (2), R21.